International Journal of Innovation and Applied Studies
ISSN 2028-9324 Vol. 42 No. 2 Apr. 2024, pp. 371-381

http://www.ijias.issr-journals.org/

Effect of physical parameters of the porous medium on natural convection in a partitioned cavity

Souleye Faye, Sidy Mactar Sokhna, Sory Diarra, and Vincent Sambou

Laboratoire Eau, Energie, Environnement et Procédés Industriels (LE3PI), École Supérieure Polytechnique de Dakar, BP: 5085, Dakar-Fann, Senegal

ABSTRACT: The aim of this article is to study numerically the influence of the physical parameters of the porous medium on the heat transfer rate. To do this, we use the Darcy-Brinkman-Forchheimer model, and a numerical tool (Ansys fluent) to solve the heat transfer and Navier-Stockes equations. The average Nusselt numbers (convective and radiative) were then determined as a function of thermal conductivity, porosity and permeability. We can deduce that as thermal conductivity increases, the heat transfer rate rises to a maximum value before decreasing. As porosity increases, radiative and convective Nusselt decrease. Finally, the transfer rate increases with increasing permeability.

KEYWORDS: Nusselt, Navier-Stockes, Darcy-Brinkman-Forchheimer, porosity, heat transfer.

1 INTRODUCTION

Natural convection in a cavity filled with a porous medium has become a very important field. It is applicable in many industrial fields such as energy storage, food processing and pharmaceuticals. Researchers have therefore carried out numerical and experimental studies to model natural convection in a porous medium.

Taking into account the forchheimer term in the equation of motion and the hydrodynamic dispersion in the thermal conductivity tensor, Ref. [1] concluded that the value of the Nusselt number decreases as the ratio of effective thermal conductivities increases.

Researches [2] have shown in a porous cavity that heat transfer rates depend on anisotropic properties by keeping vertical temperatures constant. Study [3] carried out numerical work with the Darcy-Brinkman model. They concluded that the value of the Nusselt number reaches a maximum when the Darcy number is very large. Research [4] Show that the Nusselt number varies as a function of physical parameters such as the permeability and conductivity of the walls and the thermal diffusivity of the porous material in an enclosure containing a porous medium. Study [5] studied the modelling of heat transfer from CO_2 at supercritical pressures flowing vertically in porous tubes. He concluded that the local heat transfer coefficient increases with decreasing particle diameter because the contact area between the fluid and the particles increases with decreasing particle diameter.

Researches [6] and [7] studied heat transfer in a medium. The porous material was anisotropic in conductivity and permeability. The results a] re in line with those of [8].

Researches [9] studied the effect of cavity conduction and Ra number in a numerical study of the natural convection of a square enclosure. They deduce that increasing Ra and the conductivity ratio leads to an increase in natural convection. Research [10] studied an analytical model for the energy performance of partitioned cavities. They concluded that the thermal capacity of the cavity increases with the thickness of the partitions.

Ref. [11] examined the effect of heterogeneity on free convection flow and solute transport in porous media. They observed that in fractured media, the onset of instability occurs with a lower critical Rayleigh number, meaning that fracture networks have a destabilizing effect.

Ref. [13] has shown that permeability variation has a significant influence on heat flow and heat transfer. He studied the effect of variable permeability on the vortex instability of mixed convection and the onset of convection in porous materials with vertically stratified porosity. Using an auxiliary integral equation, he demonstrated the absence of subcritical instabilities and obtained, in closed form, the global stability condition.

Ref. [14] examined convective instability, both linear and nonlinear, in a saturated porous medium, taking into account a non-zero inertia term as well as permeability variation in the vertical direction.

Ref. [15] examined the impact of variable permeability on vortex instability in horizontal natural convection flow through a porous medium adjacent to a horizontal surface. They observed that variable permeability leads to an increase in the rate of heat transfer and disturbs the flow.

Ref. [16] have carried out a numerical simulation of natural convection inside a square cavity featuring a sinusoidal cylinder of different amplitudes. Their results reveal that by increasing the amplitude (number of undulations) or changing the angle, it is possible to modify the heat transfer coefficient, which has a significant influence on the temperature and fluid field.

Ref. [17] and [18] demonstrated that porosity near a solid wall is not uniform but variable, resulting in a variation in permeability. Heterogeneity of permeability distribution can also be a feature of man-made porous materials, such as the granulate used in chemical engineering processes and the fibrous material used in fine insulation.

Ref. [18] pioneered the presentation of experimental data revealing zones of high porosity extending over two or three particle diameters from the container of a flat wall. Their results indicated that unless the D/d ratio exceeds 30, a significant variation in velocity occurs across the packed bed.

Ref. [19] studied natural thermal convection in multilayer anisotropic porous media, addressing the phenomenon of convection through these media. In the case of a large number of alternating horizontal layers, the model tends towards that of a globally homogeneous, anisotropic medium. However, for a limited number of layers, this anisotropy model presents an abrupt discontinuity due to the local appearance of convection when the local thermal porous Rayleigh number is approximately equal to 10^4.

Ref. [20] have studied combined forced and free convection on inclined surfaces immersed in porous media. Taking into account variable permeability and using the generalized momentum equation, they obtained solutions for different boundary conditions, including uniform wall temperatures and linear temperature variations at the leading edge, for both helping and opposing flows. Their analyses revealed that permeability variation exerts a strong influence on flow and heat transfer.

Ref. [21] examined the impact of heterogeneity on thermal convection in vertical porous layers. Their study highlights the effect of permeability variation on the free convection flow in a porous medium bounded by a vertical porous wall, when the permeability varies according to an exponential law in one direction. They also explored the effect of increasing permeability near an impermeable wall in a porous medium.

In the literature, we did not come across any work on the influence of the physical parameters of the medium in a partitioned cavity containing a porous medium in the case of coupled convection-radiation transfer.

The aim of this numerical study is to determine the impact of porous medium parameters such as thermal conductivity, porosity and permeability on the heat transfer rate.

To do this, we will develop a CFD model. Given the complex anisotropic conditions and the random distribution of seed shapes, we chose the Darcy-Forchheimer-Brinkman model, which links pressure drop, velocity, permeability, viscosity and porosity [22, 23, 24, 25].

In the first part, we study the influence of the thermal conductivity of the porous medium on the heat transfer rate. Next, we evaluate the heat transfer rate by varying the porosity by the Nusselt number. Finally, we investigate the effect of varying the permeability as a function of the Nusselt number

2 DESCRIPTION OF THE PROBLEM

The cavity used is a partitioned rectangle (Figure 1), with height H = 200 mm and external width L = 317 mm. Three equally spaced partitions are located between two external vertical walls. The outer walls have a thickness e = 8 mm and the inner partitions have the same finished thickness e = 3 mm. Uniform temperatures T_h = 25°C and T_c = 5°C are imposed in each of the walls at the vertical external surfaces. The inside of each cell is filled with air (Pr = 0.71). The vertical surfaces are kept adiabatic. A porous medium with porosity ε, thermal conductivity λ and permeability k is placed in the third cell.

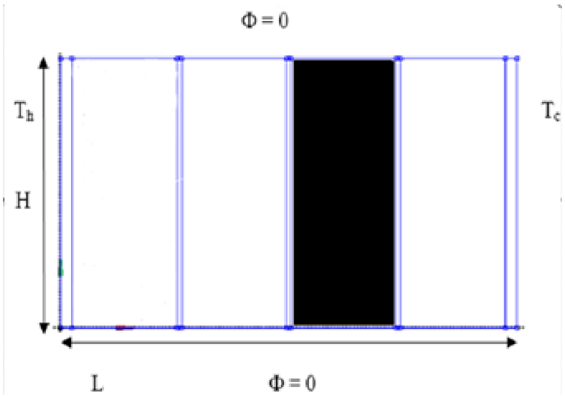

Fig. 1. System Geometry

2.1 Simplifying Assumptions And Mathematical Formulations

We assume that the fluid is Newtonian and that the flow is two-dimensional laminar and stationary. We neglect the effects of Soret and Dufour; on the other hand, the density of the fluid in the term of the forces of volume varies linearly with the temperature T according to the Bousinesq approximation [5]: $\rho = \rho_o\,[1-\beta_T\,(T-To)]$.

The equations of heat transfer, motion and continuity in a porous medium can then be written as follows.

Forming the equations dimensionally

Normalization consists in transforming the dependent and independent variables into dimensionless variables.

We obtain the following equations:

- Porous region

Continuity:

$$\frac{\partial U}{\partial X}+\frac{\partial V}{\partial Z}=0 \tag{1}$$

Move:

$$\frac{1}{\varphi}\left[\frac{1}{\varphi}\left(\frac{U\partial U}{\partial X}+\frac{V\partial U}{\partial Z}\right)\right]=-\frac{\partial P}{\partial X}+\frac{1}{\varphi}\left(\frac{\Pr}{Ra}\right)^{\frac{1}{2}}\left(\frac{\partial^2 U}{\partial X^2}+\frac{\partial^2 U}{\partial Z^2}\right)-\frac{1}{Da}\left(\frac{\Pr}{Ra}\right)^{\frac{1}{2}}U-\frac{C_f}{Da^{\frac{1}{2}}}\sqrt{U^2-V^2}U \tag{2}$$

$$\frac{1}{\varphi}\left[\frac{1}{\varphi}\left(\frac{U\partial V}{\partial X}+\frac{V\partial V}{\partial Z}\right)\right]=-\frac{\partial P}{\partial Z}+\frac{1}{\varphi}\left(\frac{\Pr}{Ra}\right)^{\frac{1}{2}}\left(\frac{\partial^2 V}{\partial X^2}+\frac{\partial^2 V}{\partial Z^2}\right)-\frac{1}{Da}\left(\frac{\Pr}{Ra}\right)^{\frac{1}{2}}V-\frac{C_f}{Da^{\frac{1}{2}}}\sqrt{U^2-V^2}V+\theta \tag{3}$$

Heat transfer:

$$\left[\left(\frac{U\partial\theta}{\partial X}+\frac{V\partial\theta}{\partial Z}\right)\right]=\lambda_{eff}\left(\Pr Ra\right)^{-\frac{1}{2}}\left(\frac{\partial^2\theta}{\partial X^2}+\frac{\partial^2\theta}{\partial Z^2}\right) \tag{4}$$

- The fluid region

Continuity:

$$\frac{\partial U}{\partial X}+\frac{\partial V}{\partial Z}=0 \tag{5}$$

Move:

$$\left[\left(\frac{U\partial U}{\partial X}+\frac{U\partial V}{\partial Z}\right)\right]=-\frac{\partial P}{\partial X}+\left(\frac{\Pr}{Ra}\right)^{\frac{1}{2}}\left(\frac{\partial^2 U}{\partial X^2}+\frac{\partial^2 U}{\partial Z^2}\right) \tag{6}$$

$$\left[\left(\frac{V\partial U}{\partial X}+\frac{V\partial V}{\partial Z}\right)\right]=-\frac{\partial P}{\partial Z}+\left(\frac{\Pr}{Ra}\right)^{\frac{1}{2}}\left(\frac{\partial^2 V}{\partial X^2}+\frac{\partial^2 V}{\partial Z^2}\right)+\theta \tag{7}$$

Heat transfer:

$$\left[\left(\frac{U\partial\theta}{\partial X}+\frac{V\partial\theta}{\partial Z}\right)\right]=\left(\Pr Ra\right)^{-\frac{1}{2}}\left(\frac{\partial^2\theta}{\partial X^2}+\frac{\partial^2\theta}{\partial Z^2}\right) \tag{8}$$

Boundary conditions:

$$\theta\left(X=0,Z\right)=0;\theta\left(X=L,Z\right)=1 \tag{9}$$

- Radiative transfer

$$\vec{\nabla}\left(I^*\left(\vec{r},\vec{s}\right),\vec{s}\right)=0 \tag{10}$$

$I^*\left(\vec{r},\vec{s}\right)$: is the radiant intensity. It is given by the following relation

$$I^*\left(\vec{r},\vec{s}\right)=I\left(\vec{r},\vec{s}\right)/\sigma T_0^4 \tag{11}$$

The dimensionless equation for the radiative flux intensity at the boundary (X=X0) is given by the following relationship:

$$I^*\left(X_0,Z\right)=\phi_{rad}^*\left(X_0,Z\right)/\prod \tag{12}$$

In the partition wall and in the walls, the equation is:

$$\left(\frac{\partial^2\theta}{\partial X^2}+\frac{\partial^2\theta}{\partial Z^2}\right)=0 \tag{13}$$

At the vertical solid-fluid interface located at X = X_0, temperatures verify:

$$\theta_s\left(X_0,Z\right)=\theta_f\left(X_0,Z\right) \tag{14}$$

The energy balance at point X = X0 (solid-fluid interface) can be deduced from this:

$$\frac{\partial\theta_s}{\partial X\ /_{X=X_0}} = Nr\phi^*_{rad}\left(X_0,Z\right)+\frac{1}{\lambda_r}\frac{\partial\theta_f}{\partial X\ /_{X=X_0}} \tag{15}$$

The radiant and conductive interaction parameter Nr is given by the following relationship:

$$N_r=\sigma T_0^4 H / \lambda_s\left(T_h-T_c\right) \tag{16}$$

The radiative flux density passing through the surface at points (X = X0, Z) is given by the following relationship:

$$\phi^*\left(X_0,Z\right)=\left(1-\varepsilon\right)\phi^*_{rad,in}\left(X_0,Z\right)+\varepsilon T^4 / T_0^4 \tag{17}$$

$\phi^*_{rad,in}$ is called the flux density of incident radiation heat on the surface. It is calculated by the following relationship:

$$\phi^*_{rad,in}=\int I^*_{in}.\vec{s}\bullet\vec{n}d\Omega \tag{18}$$

Heat transfer:

We give the convective and radiative heat transfer rates on walls and partitions by the radiative and convective Nusselt numbers are defined by:

$$Nu_{cv}\left(X_0\right)=\int_0^1\frac{\dfrac{\partial\theta_f}{\partial\theta\left(X=X_0\right)}}{\dfrac{\partial\theta_{f,cd}}{\partial X\left(X=X_0\right)}}dz \tag{19}$$

$$Nu_{rad}\left(X_0\right)=\frac{Nr}{\lambda_r}\int_0^1\frac{\phi^*_{rad}\left(X_0,Z\right)}{\dfrac{\partial\theta_{f,cd}}{\partial X\left(X=X_0\right)}}dz \tag{20}$$

θf, cd fluid temperature in the case of conduction only.

2.2 Numerical Calculation

The Navier-Stockes equations were solved using Ansys Fluent software. The mesh used is of the uniform tetrahedral type whose solution is invariant as a function of the number of elements figure 2.

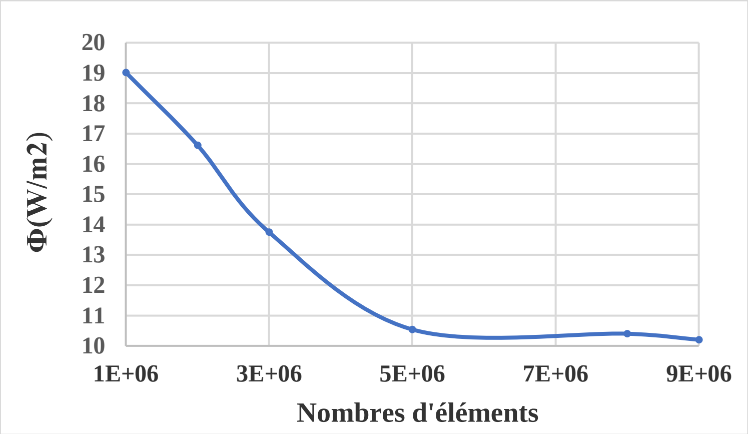

Fig. 2. Flux in function elements numbers

2.3 VALIDATION OF THE NUMERICAL MODEL

Our model is validated by comparison with the work of [16]. Considering a differentially heated square cavity modeled in Ansys Fluent. The table shows the comparison of Nusselt numbers between [16] and the present work:

Table 1. Comparison of average Nusselt numbers

Emissivity	Wang et al. (2006)	This study
$\varepsilon = 0$ Nu_c	8.852	8.87
$\varepsilon = 0.2$ Nu_c	2.337	2.306
$\varepsilon = 0.2$ Nu_r	8.399	8.348
$\varepsilon = 0.8$ Nu_c	7.873	7.763
$\varepsilon = 0.8$ Nu_r	11.208	11.077

3 RESULTS AND DISCUSSION

3.1 EFFECT OF VARYING THE THERMAL CONDUCTIVITY OF THE POROUS MEDIUM

Choosing the same boundary conditions (Ra = 10^4), Da = 10^{-5}ϕ = 0.5 and ε = 0.9, we take the previous configuration (figure 1) and vary the thermal conductivity λ of the porous medium. In the following figures, we represent a few cases of λ variation (0.1; 40; and 60).

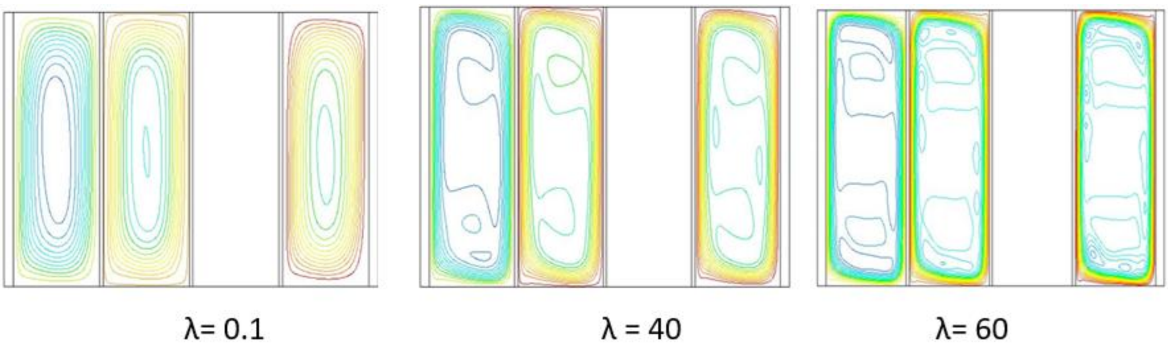

Fig. 3. Streamlines

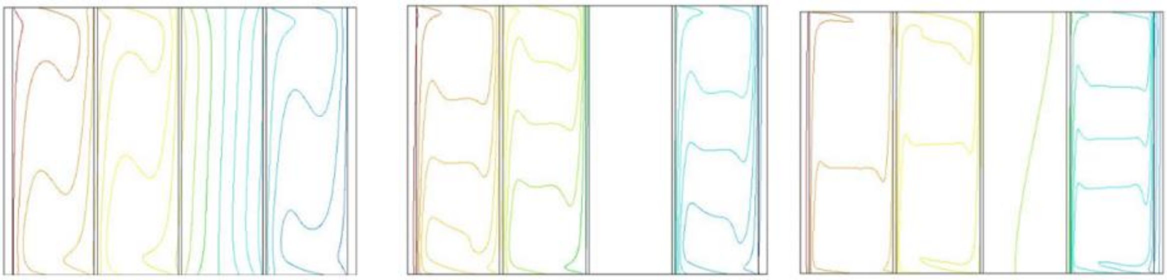

Fig. 4. Isotherms

Figure 3 shows the current lines in the system. We can see that the current lines are dissimilar. Figure 4 shows isotherms as a function of conductivity variation. We can see that thermal stratification decreases with increasing conductivity in cell 3. We can conclude that thermal conductivity has an effect on transfer rate.

Figure 5 shows the variation of the mean Nusselt number with conductivity. We divide curves 5A and 5B into two parts (one increasing and one decreasing). The increasing parts (5A and 5B) correspond to the increase in λ, which leads to a reduction in the thermal gradient between the partitions, increasing convective flow and hence Num in the cells. The decreasing parts of Num with increasing λ are due to the decrease in stratification of the thermal gradient, leading to an increase in the horizontal thermal gradient.

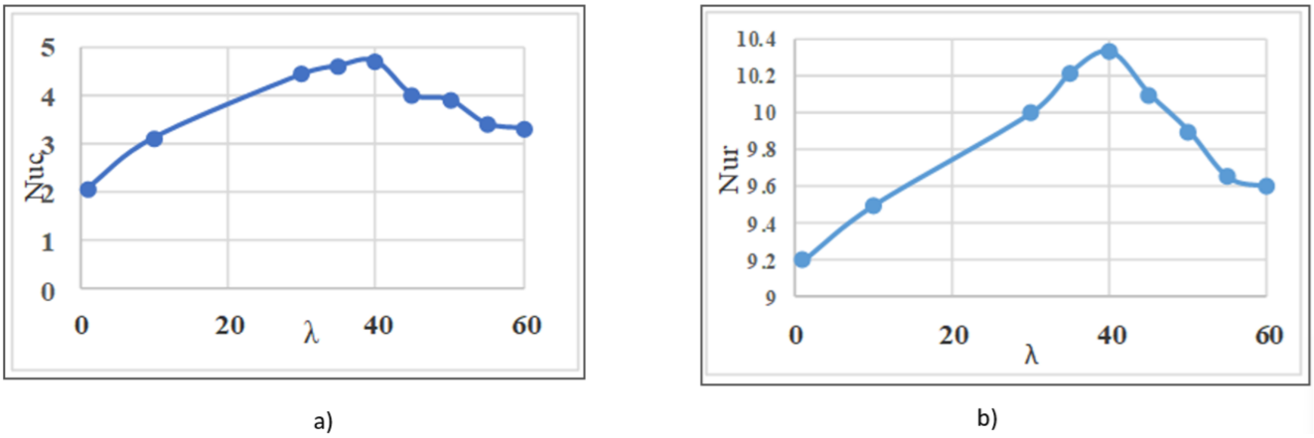

Fig. 5. Number of variation (A: convective; B: radiative) as a function of conductivity

3.2 Influence Of Porosity

Choosing the same boundary conditions (Ra = 10^4) and Da = 10^{-8}, ε = 0.9, we take the previous configuration (Figure 1) and vary the porosity ϕ of the porous medium. In the following figures, we show some cases of variations (0.1, 0.3, and 0.7).

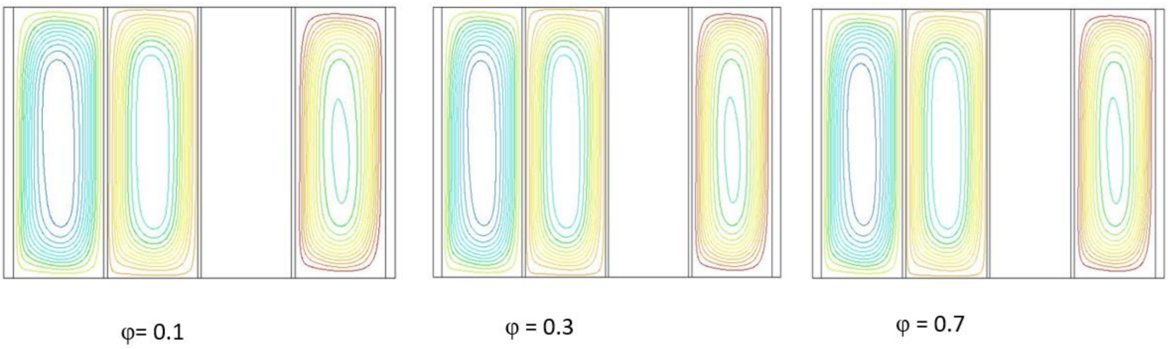

Fig. 6. Streamlines

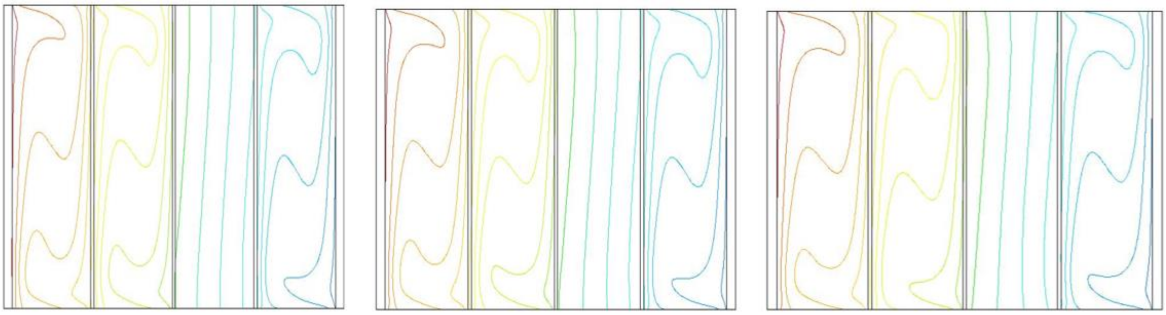

φ = 0.1 φ = 0.3 φ = 0.7

Fig. 7. Isotherms

Figure 6 shows the current lines for different values of ϕ. We can see that the shape of the current lines does not change in each case.

In the case of the isotherms shown in figure 7, the difference between the figures is that the isotherms widen with increasing in ϕ the active walls. We can therefore deduce that the intensity of the transfer flux decreases.

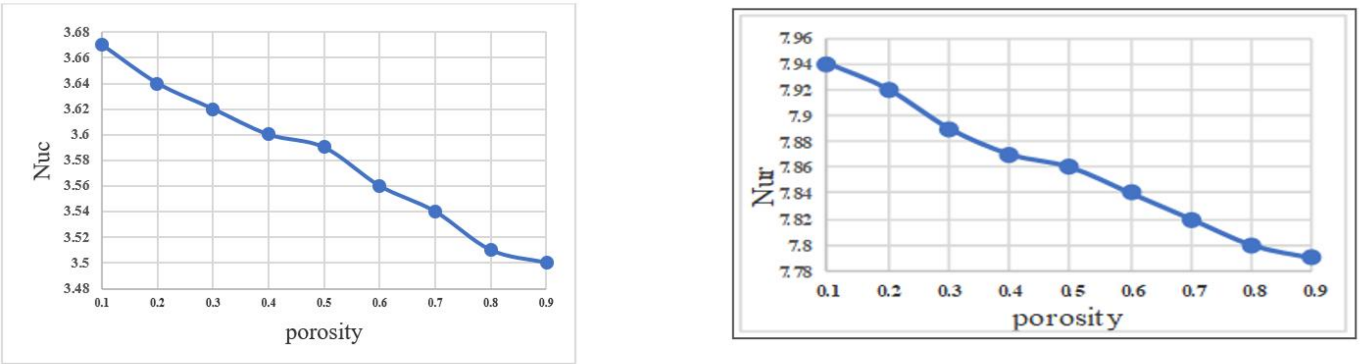

a) b)

Fig. 8. Variation in mean Nusselt number (convective a) and radiative b))

Figure 8 shows that the average Nusselt numbers (convective A and radiative B) decrease with increasing porosity value.

This shows that conductive heat transfer increases with porosity, hence the decrease in convective heat transfer.

3.3 INFLUENCE OF PERMEABILITY

Assuming the same boundary conditions (Ra = 10^4), Da = 10^{-8} and ε = 0.9, we take the previous configuration (figure 1) and vary the permeability K. In the following figures, we show a few cases of K variation ($4\ 10^{-8,}$ $4\ 10^{-6}$ and $4\ 10^{-4}$).

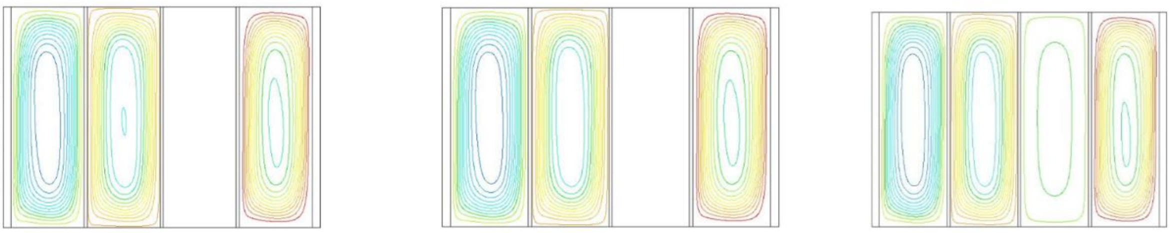

$4\ 10^{-8}$ $4\ 10^{-6}$ $4\ 10^{-4}$

Fig. 9. Streamlines

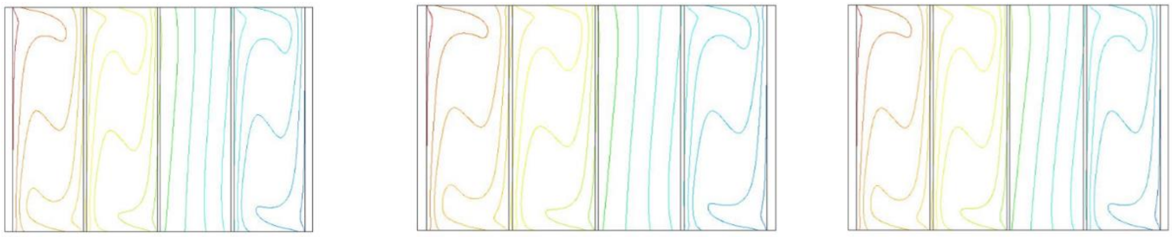

$4\ 10^{-8}$ $4\ 10^{-6}$ $4\ 10^{-4}$

Fig. 10. Isotherms

Figures 9 and 10 show current lines and isotherms for varying k permeability. For small values of K (between $4\ 10^{-8}$ and $4\ 10^{-4}$), we can see in figure 9 that the streamlines are spread out along the active walls.

For the isothermal lines in the porous medium shown in Figure 10, there is little temperature stratification. On the other hand, as permeability increases ($4\ 10^{-8}$,$4\ 10^{-6}$ and $4\ 10^{-4}$), the cells in the current lines narrow in the center of the active walls. The isotherms of the porous medium are deformed and stratification increases, so heat transfer intensifies.

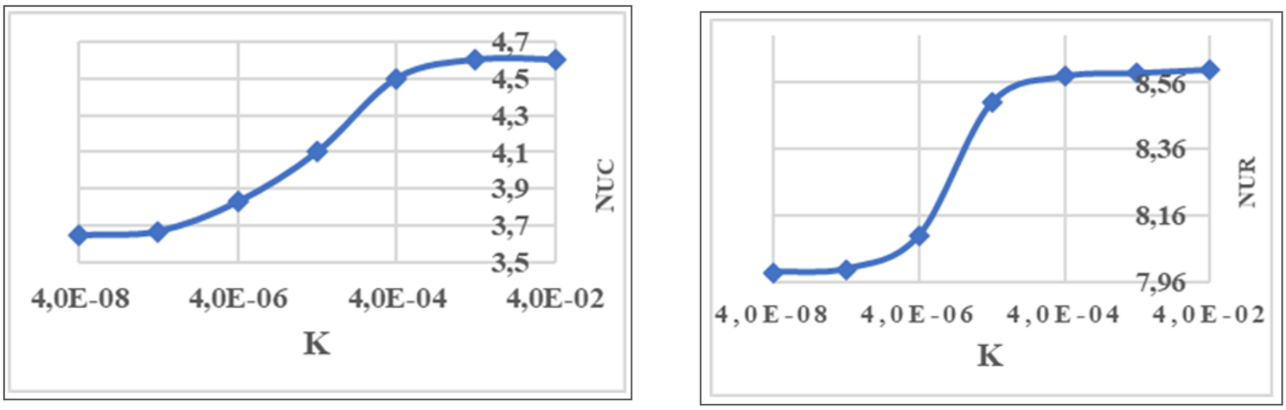

a) b)

Fig. 11. Variation in permeability as a function of average Nusselt number (a) convective and (b) radiative

Figure 11 shows the variation in heat transfer rate as a function of the Nusselt number of the permeability anisotropy. The figure can be broken down into three parts: two almost constant parts at the beginning and towards the end, and an increasing part between the two preceding phases. We can see that convective and radiative heat transfer rates are low when k is between ($4\ 10^{-8}$ and $4\ 10^{-6}$). This is due to a low flow rate, as the permeability is very low, so the flow is almost diffusive.

When k is between ($4\ 10^{-6}$ and $4\ 10^{-4}$), the progression of the Nusselt number is very rapid as the value of k increases. The flow regime is said to be moderate. When k is between ($4\ 10^{-6}$ and $4\ 10^{-4}$), the progression is almost constant with the variation in K: this is the complete boundary layer regime.

4 CONCLUSIONS

The aim of the present work is to determine the influence of the physical parameters of the porous medium in a partitioned cavity on heat transfer using numerical simulation.

The Darcy-Brinkman-Forchheimer model was chosen, and a numerical tool was used to solve the heat transfer and momentum equations. We then determined the average Nusselt numbers (convective and radiative) as a function of the porous medium parameters. It can be deduced that as conductivity increases, the heat transfer rate rises to a maximum value before decreasing. The heat transfer rate then decreases with increasing porosity. Finally, the heat transfer rate increases with increasing permeability.

We plan to continue the work by adding porous medium to the other cells, then increasing the number of partitions in the cavity.

NOMENCLATURE

Cf Forchheimer coefficient
Da Darcy numbers
g Acceleration due to gravity (ms^{-2})
H Channel height (m)
I Radiation intensity (Wm^{-2})
K Permeability
L Width (m)
Nu Nusselt number
P Pressure (Pa)
Pr Prandtl number ϑ/α
Ra Rayleigh number $g\beta(T_h - T_c)\, H^3/\vartheta\alpha$
T Temperature (K)
U, *V* Dimensionless velocity components
x, z Cartesian coordinates (m)
X, Z Dimensionless Cartesian coordinate
βT Thermal expansion coefficient (K^{-1})
Θ Dimensionless temperature (K)
ε Emissivity
λ Thermal conductivity ($Wm\text{-}1K^{-1}$)
ρ Density (kgm^{-3})
Φ Heat flux density (Wm^{-2})
φ Porosity
c Cold
cd Conduction
cv Convection
rd Radiation
h Hot
m Average
w Wall

REFERENCES

[1] L.E. Howle and J.G. Georgiadis, 'Natural Convection in Porous Media with Anisotropic Dispersive Thermal Conductivity', International Journal of Heat and Mass Transfer, Vol. 37, N°7, pp. 1081 - 1094, 1994.
[2] R. Bennacer, A. Tobbal, H. Beji and P. Vasseur, 'Double Diffusive Convection in a Vertical Enclosuren Filled with Anisotropic Porous Media', International Journal of Thermal Sciences, Vol. 40, N°1, pp. 30 - 41, 2001.
[3] W. Zheng and L. Robillard, 'Convection in a Square Cavity Filled with in Anisotropic Porous Medium Saturated with Water Near 4 °C', International Journal of Heat and Mass Transfer, Vol. 44, N°18, pp. 3463 - 3470, 2001.
[4] F. Chen and J.W. Lu, 'Onset of Salt-Finger Convection in an Anisotropic and Inhomogeneous Porous Media', International Journal of Heat and Mass Transfer, Vol. 35, N°12, pp. 3451 - 3464, 1992.
[5] Masoud Haghshenas Fard, CFD modeling of heat transfer of CO2 at supercritical pressures flowing vertically in porous tubes. International Communications in Heat and Mass Transfer 37 (2010) 98-102.
[6] K.L. Walker and G.M. Homsy, 'Convection in a Porous Cavity', Journal of Fluid Mechanics, Vol. 87, N°3, pp. 449 - 474, 1978.
[7] G.S. Shiralkar, M. Haajizadeh and C.L. Tien, 'Numerical Study of High Rayleigh Number Convection in a Vertical Porous Enclosure', Numerical Heat Transfer, Part B, Fundamentals: Vol. 6, N°2, pp. 223 - 234, 1983.
[8] J. Ni et C. Beckermann, 'Natural Convection in a Vertical Enclosure Filled With Anisotropic Porous Media', Journal of Heat Transfer, Vol. 113, N°4, pp. 1033 - 1037, 1991.
[9] M. Mobedi, Conjugate natural convection in a square cavity with finite thickness horizontal walls, Int. Communication in Heat and Mass Transfer, vol. 35, pp.503-513, 2008.
[10] Vincent Sambou, Berangere Lartigue, Franc xoise Monchoux et Mamadou Adj; Modélisation de la performance thermique des enceintes cloisonnées remplies d'air: Effets de la géométrie et des propriétés thermiques. Journal of Building Physics. 2016, Vol. 39 (4) 321-341.

[11] Shafabakhsh, P., Fahs, M., Ataie-Ashtiani, B., Simmons, C.T. " Unstable density-driven flow in fractured porous media: the fractured elder problem ". Fluids 4, 168 (2019).

[12] Haddad, S.A.M. " Thermal convection in a Darcy porous medium with anisotropic spatially varying permeability ". Acta Appl. Math. 132, 359–370 (2014).

[13] Hassanien, I.A., Salama, A.A., Elaiw, A.M. " Variable permeability effect on vortex instability of a horizontal natural convection flow in a saturated porous medium with variable wall temperature ". J. Appl. Math. Mech. 84, 39–47 (2004).

[14] Roblee, L.H.S., Baird, R.M., Tierney, J.W. " Radial porosity variations in packed beds ". AIChE J. 4, 460–464 (1958).

[15] Benenati, R.F., Brosilow, C.B. " Void fraction distribution in beds of spheres ". AIChE J. 8, 359–361 (1962).

[16] Schwartz, C.E., Smith, J.M. " Flow distribution in packed beds ". Ind. Eng. Chem. 45, 1209–1218 (1953).

[17] Chandrasekhara, B.C., Namboodiri, P.M.S., Hanumanthappa, A.R. " Similarity solutions for buoyancy induced flows in a saturated porous medium adjacent to impermeable horizontal surfaces ". Wärme-Und Stoffübertragung 18, 17–23 (1984).

[18] Singh, P., Misra, J.K., Narayan, K.A. " Free convection along a vertical wall in a porous medium with periodic permeability variation ". Int. J. Numer. Anal. Methods Geomech. 13, 443–450 (1989).

[19] McKibbin, R., Tyvand, P.A. " Anisotropic modelling of thermal convection in multilayered porous media ". J. Fluid Mech. 118, 315–339 (1982).

[20] G. Neale, «Degree of Anisotropy for Fluid Flow and Diffusion (Electrical Conduction) Through An.

[21] J.F. Epherre, «Critère d'application de la Convection Naturelle dans une Couche Poreuse Anisotrope», Revue Générale de Thermique, Vol. 168, pp. 949 - 950, 1975. isotropic Porous Media«, AIChE Journal, Vol. 23, N°1, pp. 56 - 62, 1977.

[22] P.A. Tyvand, «Heat Dispersion Effect on Thermal Convection in Anisotropic Porous Media», Journal of Hydrology, Vol. 34, N°3-4, pp. 335 - 342, 1977.

[23] R. McKibbin et P.A. Tyvand, «Anisotropic Modeling of Thermal Convection in Multilayered Porous Media», Journal of Fluid Mechanics, Vol. 118, N°1, pp. 315 - 339, 1982.

[24] J. Ni et C. Beckermann, «Natural Convection in a Vertical Enclosure Filled With Anisotropic Porous Media», Journal of Heat Transfer, Vol. 113, N°4, pp. 1033 - 1037, 1991.